



CHORUS

This is the accepted manuscript made available via CHORUS. The article has been published as:

Experimental observation of the lowest levels in the photoassociation spectroscopy of the 0_{g}^{-} purely-long-range state of Cs_{2}

Yichi Zhang, Jie Ma, Jizhou Wu, Lirong Wang, Liantuan Xiao, and Suotang Jia

Phys. Rev. A **87**, 030503 — Published 12 March 2013

DOI: [10.1103/PhysRevA.87.030503](https://doi.org/10.1103/PhysRevA.87.030503)

Experimental observation of missing lowest levels in the photoassociation spectroscopy of the 0_g^- pure long-range state of Cs_2

Yichi Zhang, Jie Ma*, Jizhou Wu, Lirong Wang, Liantuan Xiao, and Suotang Jia
State Key Laboratory of Quantum Optics and Quantum Optics Devices,
Laser Spectroscopy Laboratory, College of Physics and Electronic Engineering,
Shanxi University, Taiyuan 030006, People's Republic of China

We have experimentally observed two missing lowest vibrational levels of Cs_2 0_g^- purely long-range states. The photoassociation spectroscopy of ultracold cesium atoms with rotational structure presents clear identification of missing lowest levels. Values of radiative lifetimes $\tau_{3/2} = 30.41 \pm 0.06$ ns and $\tau_{1/2} = 34.81 \pm 0.07$ ns of the $6p^2P_{1/2}$ and $6p^2P_{3/2}$ atomic levels and van der Waals coefficient $C_6 = 6852 \pm 25$ a.u. of ground state cesium molecule are extracted, respectively.

PACS number(s): 33.20.-t, 37.10.Mn, 34.20.-b, 34.10.+x

Research on cold and ultracold molecules received large attention in the last decade due to important advances and potentially new application in several domains like quantum computing [1], few body physics and physical chemistry [2]. The techniques that have produced up to now molecules in the ultracold temperature range mainly are magnetoassociation (MA) [3] and photoassociation (PA) [4]. PA spectroscopy of ultracold atoms has become a powerful tool for investigation of the so-called long-range molecules with classical outer turning points of several to hundreds nanometers. In the long-range molecules, properties of the molecular states are closely related to properties of their constituent atoms. A special class of long-range molecules is called a purely long-range (PLR) molecule. It has a classical inner turning point at a long internuclear distance where the short-range interaction due to the overlap of atomic electron clouds is negligible.

The spin-orbit coupling causes an avoided crossing between attractive and repulsive potentials correlating to different asymptotes. With increasing precision of the experiments, highly sensitive detection methods have brought significant progress in the domain of precision measurements for the PLR cesium molecule (Cs_2), for instance, resonant four-body interaction in cold cesium Rydberg atoms [5], absolute frequency stabilization to cesium atom molecular hyperfine transitions [6], the C_6 and a_T values of Cs_2 obtained in Ref. [7]. In these ultracold Cs_2 experiments, the double-well structure of the 0_g^- molecular state correlated to the $6S_{1/2}+6P_{3/2}$ dissociation limit is a key feature in the process of forming ultracold molecules. The reliable description of this state is crucial, as the double-well structure of the PLR 0_g^- state appears as a suitable intermediate step in the course of the formation of ground state molecules in their absolute ground state [8]. Photoassociation spectroscopy of Cs_2 0_g^- PLR state had been obtained by Pillet *et al.* using ionization detection technique in 1999 [9]. Another feasible technique to directly detect the excited molecular state levels is trap-loss detection by monitoring the fluorescence yield from the trapped atoms described by M. Pichler *et al.* [10]. In these pioneering experiments, they

obtained the “lowest” vibrational level $v' = 0$ in Cs_2 0_g^- state by directly observation until the vibrational series broken off. The PA spectroscopy of PLR 0_g^- state of ultracold Cs_2 has been theoretically interpreted by Olivier Dulieu *et al.* [11, 12]. They provided a precision analytical expression for the external well of the 0_g^- potential curve and convinced atomic lifetimes. It is very important to note that Dulieu and co-workers predicted two levels energetically below the “lowest” level $v' = 0$. However, such two missing lowest levels have not been experimentally observed so far, since the overlap between the two missing lowest levels states with the triplet ground state wave function is expected to be very small and it is difficult to observe the PA lines of missing levels with a very low intensity [11, 12]. If these two missing lowest levels exist, the pioneering lowest vibrational level $v' = 0$ is actually $v = 2$, numerous experimental and theoretical studies which based on 0_g^- vibrational levels, besides, spectroscopy and potential curve should be modified [6–8, 13].

In this paper, we report the experimental observation of the missing lowest levels of ultracold PLR cesium molecules by carrying out three-dimensional modulation PA spectroscopy. Resolved ro-vibrational spectra of the PLR $0_g^- (6P_{3/2})$ state are obtained. The bound energy data of missing lowest levels are compared to theoretical predictions. We represent the potential curve with these new data by an analytical asymptotic approach. Values of the radiative lifetimes of the $6p^2P_{1/2}$ and $6p^2P_{3/2}$ atomic levels and van der Waals coefficient C_6 of ground state are obtained.

The details of the experimental setup have been schematically depicted in [6]. The sample of ultracold atoms was produced in a standard vapor-loaded ^{133}Cs magneto-optical trap (MOT) [14]. The trapping and repumping laser frequencies were locked to the Cs atomic transition $6S_{1/2}(F=4) \rightarrow 6P_{3/2}(F'=5)$ and $6S_{1/2}(F=3) \rightarrow 6P_{3/2}(F'=4)$, respectively. Fig.1(a) shows the formation and modulation scheme of photoassociative Cs molecules in the $0_g^- (6P_{3/2})$ state. The PA laser excites a pair of colliding Cs atoms into a PLR state. Ground state ($a^3\Sigma_u^+$) molecules are formed from these

excited molecules followed by spontaneous decay from the 0_g^- state. In PA experiments, the response time of the MOT is usually rather slow (~ 1 s), thus it requires slow scanning rate of the PA laser frequency. Therefore, a fast and effective modulation of the number of trapped cold atoms is difficult. We employ a coupling laser as an independent modulation medium in order to controllably modulate the fluorescence of the trapped atoms [14, 15]. The coupling laser beams, provided by a diode laser, are introduced into the center of MOT strictly along the directions of the trapping laser beams. For sine wave modulation, the instantaneous frequency of the coupling laser is $\nu(t) = \nu_0 - m \cos(2\pi\omega t)$, where ν_0 is the carrier frequency, m is the modulation index, and ω is the modulation frequency.

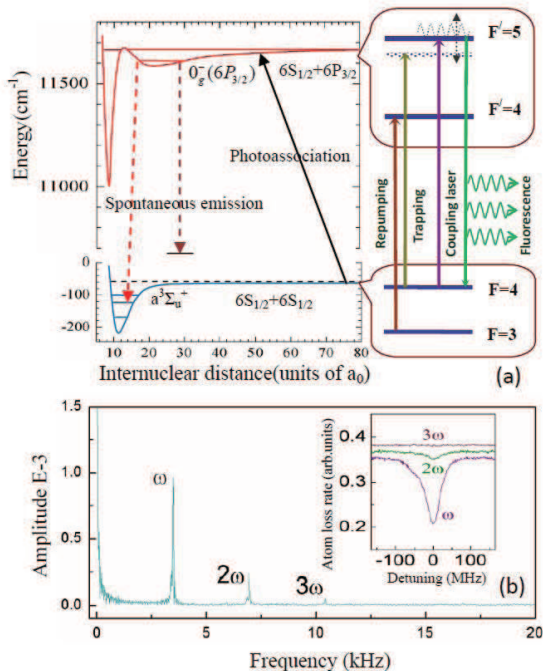


FIG. 1. (color online) (a) Detection scheme of the improved three dimensional fluorescence modulation spectroscopy of the 0_g^- state of Cs_2 dissociating towards the $(6S_{1/2} + 6P_{3/2})$ limit. (b) Noise power spectra of cold atomic fluorescence versus modulation frequency. The inset shows the low frequency part.

The intensity of the coupling laser is set to be very weak (10% of the trapping laser power), which is the best power with little trapped cold atoms be heated to escape from MOT despite the maximum absorption. Note that the coupling laser frequency is the same as the trapping laser with a red detuning of ~ 10 MHz relative to the Cs atomic resonant frequency in our measurement. We apply the optimal values of modulation index and frequency, $m = 2$ and $\omega = 3.3$ kHz. Fig. 1(b) shows the noise power spectra of the cold atoms' fluorescence in MOT and the electronic noise of the detection system. The modulation signal and its high-order terms are

clearly demonstrated. The demodulated signal in the first-order (the purple curve in the inset of Fig. 1(b)) corresponds to a best signal-to-noise ratio (SNR) of 14.5. Therefore, we take first-order ω as the demodulation reference frequency.

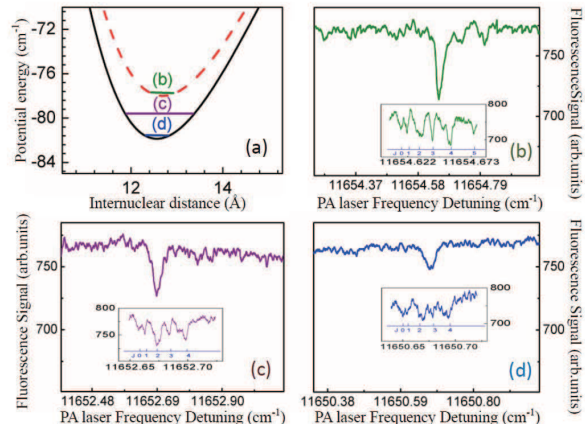


FIG. 2. (color online) (a) Schematic of vibrational levels ($v = 2$, $v = 1$, and $v = 0$) in potential curve of 0_g^- external well are indicated by straight olive, purple, and blue, respectively. The vibrational spectroscopy of $v = 2$, $v = 1$, and $v = 0$ are shown in (b), (c), and (d). The inset of (b), (c), and (d) show the rotational spectroscopy for $v = 2$, $v = 1$, and $v = 0$, respectively.

Fig. 2(a) describes the position of vibrational levels ($v = 2$, $v = 1$, and $v = 0$) in the Cs_2 0_g^- external well by theory predictions [11]. In our experiment, the PA laser frequency was tuned to about 11654.6 cm^{-1} for observing the spectra of $v = 2$ (olive line), which was recognized as the lowest vibrational level $v' = 0$ in the previous experiments [6, 9, 10]. The two deeper levels are two missing lowest levels $v = 1$ and $v = 0$ (purple and blue lines, shown in Fig. 2(a)), which theoretically predicted by O. Dulieu, *et al.* are firstly been observed in our experiment. Well resolved PA spectra of the vibrational quantum number $v = 2$ of the 0_g^- ($6P_{3/2}$) PLR state of Cs_2 , whose detuning is red shifted for $\sim 77.5 \text{ cm}^{-1}$ from the $6S_{1/2} + 6P_{3/2}$ dissociation limit, is shown in Fig. 2(b). Rotationally resolved trap loss spectra for $v = 2$ of Cs_2 PLR state up to $J=5$ is shown in the inset of Fig. 2(b). The difference (0.42 cm^{-1}) of rotational level energies between our spectra and the experimental spectra of Ref. [16] stems from the difference in calibration benchmark of PA laser frequency. The line shape of the spectra for the different J is the same as reported in Ref. [17]. As shown in Fig. 2(c), the PA line intensity of the vibrational level $v = 1$ of the Cs_2 0_g^- PLR state is very small as expected to be, whose detuning is red shifted for $\sim 79.5 \text{ cm}^{-1}$ from the $6S_{1/2} + 6P_{3/2}$ dissociation limit. Fig. 2(d) demonstrates the observed PA spectra of the missing lowest vibrational level $v = 0$ of the Cs_2 0_g^- PLR state, whose detuning is red shifted for $\sim 81.6 \text{ cm}^{-1}$ from the $6S_{1/2} + 6P_{3/2}$ dissociation limit. The signal-to-noise

ratio of rotational spectra is too poor to distinguish rotational lines $J = 0$ and $J = 1$, shown in the inset of Fig. 2(d), because of the extremely tiny Franck-Condon factor. The experimental energies of the $v=2$ and missing levels of the Cs_2 PLR state are shown in Table I. The uncertainty is mainly due to a possible systematic error in the process of fitting and error in the determination of the resonant line position.

TABLE I. The experimental energies of the $v=2$ and missing levels of the Cs_2 0_g^- PLR state.

v	$E(J=0)(\text{cm}^{-1})$	$E(J=1)(\text{cm}^{-1})$	$E(J=2)(\text{cm}^{-1})$	$E(J=3)(\text{cm}^{-1})$	$E(J=4)(\text{cm}^{-1})$	$E(J=5)(\text{cm}^{-1})$
0			11650.6667	11650.6801	11650.6970	
1	11652.6574	11652.6615	11652.6707	11652.6833	11652.6993	
2	11654.6171	11654.6213	11654.6297	11654.6423	11654.6588	11654.6800

For represent the potential energy curve with the missing lowest levels of the Cs_2 0_g^- PLR state, we have used the analytical asymptotic approach [11]. In Hund's case-c representation, the 0_g^- ($6S_{1/2} + 6P_{3/2}$) double-well state arises from the mixing between the $^3\Pi_g(6S + 6P)$ and $^3\Sigma_g^+(6S + 6P)$ Hund's case-a states. The 2×2 matrix of the Hamiltonian describing this mixing can be written as [11]:

$$H = \begin{pmatrix} V^\Pi(R) - \Delta^{\text{III}}(R) & \frac{\sqrt{2}M^2\epsilon}{9R^3} + \Delta^{\text{II}\Sigma}(R) \\ \frac{\sqrt{2}M^2\epsilon}{9R^3} + \Delta^{\text{II}\Sigma}(R) & V^\Sigma(R) \end{pmatrix} \quad (1)$$

where the $V^\Pi(R)$ and $V^\Sigma(R)$ are the $^3\Pi_g$ and $^3\Sigma_g^+$ asymptotic potentials, $\Delta^{\text{III}}(R)$ and $\Delta^{\text{II}\Sigma}(R)$ are the R -dependent spin-orbit interaction within the $^3\Pi_g$ manifold and between the $^3\Pi_g$ and $^3\Sigma_g^+$ states, respectively. The asymptotic potentials $V^\Pi(R)$ and $V^\Sigma(R)$ are given by

$$V^\Sigma(R) = -\frac{C_3^\Sigma}{R^3} \left(1 + \frac{2\epsilon}{3}\right) - \frac{C_6^\Sigma}{R^6} - \frac{C_8^\Sigma}{R^8} + V_{exch}^\Sigma, \quad (2)$$

$$V^\Pi(R) = -\frac{C_3^\Pi}{R^3} \left(1 + \frac{4\epsilon}{3}\right) - \frac{C_6^\Pi}{R^6} - \frac{C_8^\Pi}{R^8} + V_{exch}^\Pi. \quad (3)$$

The relativistic effects are introduced in these equations as a small correction to the coefficients of the R^{-3} terms [11, 12], the parameter ϵ characterizing the ratio of the squared transition moments $M_{1/2}$ and $M_{3/2}$ corresponding to the relativistic $P_{1/2}$ and $P_{3/2}$ states

$$\mathfrak{R} = \frac{(M_{3/2})^2}{(M_{1/2})^2} = \frac{2\tau_{1/2}(\lambda_{3/2})^3}{\tau_{3/2}(\lambda_{1/2})^3} = \frac{2}{(1 + \epsilon)^2}. \quad (4)$$

where $(\lambda_{3/2})^{-1} = 11732.3071\text{cm}^{-1}$ and $(\lambda_{1/2})^{-1} = 11178.2682\text{cm}^{-1}$ are the $6p_{3/2,1/2} \rightarrow 6s$ transition wave numbers [12]. The M^2 coefficient in Eq.(1) is related to the $C_3^{\Sigma/\Pi}$ coefficients by

$$C_3^\Pi = -\frac{C_3^\Sigma}{2} = -\frac{M^2}{3}. \quad (5)$$

and it is related to the relativistic atomic transition moment corresponding to $j = 3/2$ by

$$M^2 = \frac{3}{4}(M_{3/2})^2. \quad (6)$$

The $V_{exch}^{\Sigma/\Pi}$ is the exchange energy between the two atoms [18]. The spin-orbit interaction terms are given by

$$\Delta^{\text{III}}(R) = \frac{\Delta E_{fs}}{3} \tanh(A^{\text{III}}R), \quad (7)$$

$$\Delta^{\text{II}\Sigma}(R) = \frac{\sqrt{2}\Delta E_{fs}}{3} \tanh(A^{\text{II}\Sigma}R), \quad (8)$$

where $\Delta E_{fs} = 554.039 \text{ cm}^{-1}$ is the Cs $6p$ fine structure splitting [11, 12].

Diagonalization of the 2×2 matrix of Eq. (1) yields an analytical expression for the potential curve of the Cs_2 0_g^- external well. We used a minimization procedure based on the so-called generalized simulated annealing (GSA) method to minimize root-mean-squared (rms) deviation [19]. Nine parameters were at first considered, as in Ref. [11]: the squared atomic transition moment M^2 , the relativistic parameter ϵ , the multipole coefficients C_6^Σ , C_6^Π , C_8^Σ , C_8^Π , the values A^{III} and $A^{\text{II}\Sigma}$ of the spin-orbit variational parameters, and the exchange amplitude $a_{6s}a_{6p}$.

TABLE II. Result of the present work, together with the result of Ref. [11] and with some theoretical values. The standard deviation of the parameters is indicated in parentheses.

parameters	this paper	Ref. [11]	theory
$M^2(10^5 \text{ cm}^{-1} \text{ \AA}^3)$	9.808(1)	9.806	10.22 [20]
$C_6^\Pi(10^7 \text{ cm}^{-1} \text{ \AA}^6)$	5.78 (1)	5.869	5.701 [20]
$C_6^\Sigma(10^7 \text{ cm}^{-1} \text{ \AA}^6)$	8.798(1)	8.778	8.381 [20]
$C_8^\Pi(10^9 \text{ cm}^{-1} \text{ \AA}^8)$	3.332 (3)	3.522	3.045 [20]
$C_8^\Sigma(10^9 \text{ cm}^{-1} \text{ \AA}^8)$	17.261 (3)	17.525	6.802 [20]
$a_{6s}a_{6p}$	0.04150 (4)	0.04512	0.05479[18]
$\epsilon 10^{-3}$	4.79 (2)	4.81	

In order to obtain the best possible fit, we restricted the experimental data to the 76 lowest vibrational levels from $v = 0$ to $v = 75$ to the rotational level $J = 2$, which corresponds to and by far the most intense lines of the observed rotational progression involving $J = 0 - 6$. The experimental energy levels lying in the Cs_2 0_g^- external well are produced with a rms of 0.0035 cm^{-1} . The Table II presents the asymptotic parameters obtained from this analysis, together with the result of Ref. [11] and with some theoretical values [18, 20]. We determine a standard deviations on the parameters by fitting 100 sets of experimental energies, obtained after adding a random distribution of the experimental error bar ($\pm 0.006\text{cm}^{-1}$) over the measured energies. The values obtained for the

parameters $A^{\text{II}\Sigma}$ and $A^{\text{III}\Pi}$ were rather large, so that the spin-orbit interaction was hardly varying in the R range of the 0_g^- external well. Thus, we therefore suppressed these two parameters by giving them fixed infinite values. The adjusted values for the ϵ , M_2 , C_3 and C_6 are not very different from the ones of Ref. [11] and are in good agreement with the theoretical predictions (with a relative difference smaller than 5%). The value of the parameter $\epsilon = 4.79 * 10^{-3}$ is slightly smaller compared to the values in Ref. [11]. The differences in the value of C_8^{II} is closer to the value in Ref. [11], a little bigger compared to the theoretical value of Ref. [20] (with a relative difference smaller than 9%). The value of C_8^{Σ} is a little smaller than the one in Ref. [11] but still more than twice as large as the theoretical values of Ref. [20]. The value obtained for the asymptotic exchange amplitude $a_{6s}a_{6p}$ is closer to the one in Ref. [11] and the theoretical value of Ref. [18]. The Cs_2 0_g^- ($6P_{3/2}$) external well potential curve is represented with and without two missing lowest levels, respectively, as shown in Fig. 3. The potential minimum with two missing lowest levels (black full lines) is obtained at $R_{\text{min}}=12.52(1) \text{ \AA}$, which is slightly smaller than without two missing lowest levels (red dashed lines $R_{\text{min}}=12.69(1) \text{ \AA}$) and with a minimum value $E_{\text{min}}=-81.864(3) \text{ cm}^{-1}$, which is notably deeper than the red dashed one ($E_{\text{min}}=-78.004(5) \text{ cm}^{-1}$).

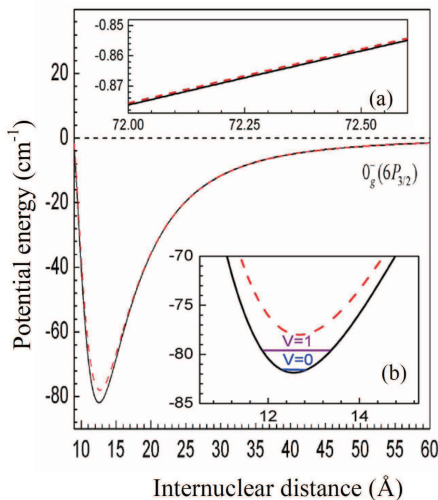


FIG. 3. (color online) Potential curve of the PLR 0_g^- ($6P_{3/2}$) external well of Cs_2 , obtained with the missing lowest levels $v = 1$ and $v = 0$ (black full lines) and without the missing lowest levels (red dashed lines). Insets (a) and (b) emphasize the differences between the two curves in the region at the large and minimum distance, respectively.

The most important result of present work is the determination of the lifetimes $\tau_{3/2}$ and $\tau_{1/2}$ of the $6P_{3/2}$ and $6P_{1/2}$ atomic levels, respectively [11]. The atomic lifetimes values can be deduced from the adjusted parameter M^2 by

$$\tau_{3/2} = \frac{9\hbar}{4M^2} \left(\frac{\lambda_{3/2}}{2\pi} \right)^3, \quad (9)$$

$$\tau_{1/2} = \tau_{3/2} \left(\frac{\lambda_{1/2}}{\lambda_{3/2}} \right)^3 \frac{1}{(1 + \epsilon)^2}. \quad (10)$$

where the M^2 and ϵ corresponding to the fit of Table I, $\tau_{3/2} = 30.44 \pm 0.06$ ns and $\tau_{1/2} = 34.81 \pm 0.07$ ns, in agreement with $\tau_{3/2} = 30.41 \pm 0.30$ ns and $\tau_{1/2} = 34.82 \pm 0.36$ ns [11], $\tau_{3/2} = 30.41 \pm 0.10$ ns and $\tau_{1/2} = 34.75 \pm 0.07$ ns [21], and $\tau_{3/2} = 30.39 \pm 0.06$ ns and $\tau_{1/2} = 34.80 \pm 0.07$ ns [22]. The relative uncertainty on these value is the same as the one on M^2 of the order of 0.2%. Moreover, we can use the method of Ref. [23] to deduce the C_6 coefficient by

$$C_6 = M_{1/2}^4 \xi_P + M_{1/2}^2 \xi_x + \xi_r, \quad (11)$$

where ξ_P , ξ_x , and ξ_r are coefficients evaluated by [23]. From our value of $\tau_{3/2}$ and \mathfrak{R} , we can derive $M_{1/2}$ and finally obtain $C_6 = 6852 \pm 25$ a.u., in good agreement with the values 6850 ± 140 a.u. [11], 6860 ± 25 a.u. [24] and 6846 ± 16 a.u. [25]. The uncertainty of 0.36% in C_6 is estimated by considering the uncertainties on the ξ_P , ξ_x , and ξ_r parameters reported in Ref. [24], and the one on \mathfrak{R} from our analysis.

In conclusion, we report the observation of the predicted levels of PLR Cs_2 by PA spectroscopy, which are theoretically predicted by Olivier Dulieu, *et al.* [11]. The vibration quantum numbers of Cs_2 0_g^- state are modified as $v = v' + 2$.

The authors gratefully thank Xiaomeng Liu (Shanxi University, China) and Prof. Olivier Dulieu (Laboratory Aimé Cotton, France) for many valuable discussions. This research is sponsored by the 973 program (No.2012CB921603), the 863 program (No.2011AA010801), the international science & technology cooperation program of China (No.2011DFA12490), NSF of China (Nos.61008012 and 10934004), and RFDP (No.2011AA010801).

[1] D. DeMille, Phys. Rev. Lett. **88**, 067901 (2002).

[2] B. Wunsch, N. T. Zinner, I. B. Mekhov, S. J. Huang, D. W. Wang, and E. Demler, Phys. Rev. Lett. **107**, 073201 (2011).

[3] O. Dulieu and C. Gabbanini, Rep. Prog. Phys. **72**, 086401 (2009).

[4] K. M. Jones, E. Tiesinga, P. D. Lett, and P. S. Julienne, Rev. Mod. Phys. **78**, 483 (2006).

- [5] J. H. Gurian, P. Cheinet, P. Huillery, A. Fioretti, J. Zhao, P. L. Gould, D. Comparat, and P. Pillet, *Phys. Rev. Lett.* **108**, 023005 (2012).
- [6] J. Ma, L. R. Wang, Y. T. Zhao, L. T. Xiao, and S. T. Jia, *Appl. Phys. Lett.* **91**, 161101 (2007).
- [7] C. Drag, B. Laburthe Tolra, B. T. Jampens, D. Comparat, M. Allegrini, A. Crubellier, and P. Pillet, *Phys. Rev. Lett.* **85**, 1408 (2000).
- [8] I. Manai, R. Horchani, H. Lignier, P. Pillet, D. Comparat, A. Fioretti, and M. Allegrini, *Phys. Rev. Lett.* **109**, 183001 (2012).
- [9] A. Fioretti, D. Comparat, C. Drag, C. Amiot, O. Dulieu, F. Masnou-Seeuws, and P. Pillet, *Eur. Phys. J. D* **5**, 389 (1999).
- [10] M. Pichler, H. M. Chen, and W. C. Stwalley, *J. Chem. Phys.* **121**, 6779 (2004).
- [11] N. Bouloufa, A. Crubellier, and O. Dulieu, *Phys. Rev. A* **75**, 052501 (2007).
- [12] C. Amiot, O. Dulieu, R. F. Gutterres, and F. Masnou-Seeuws, *Phys. Rev. A* **66**, 052506 (2002).
- [13] L. Pruvost and H. Jelassi, *J. Phys. B: At. Mol. Opt. Phys.* **43**, 125301 (2010).
- [14] J. Z. Wu, J. Ma, Y. C. Zhang, Y. Q. Li, L. R. Wang, Y. T. Zhao, G. Chen, L. T. Xiao, and S. T. Jia, *Phys. Chem. Chem. Phys.* **13**, 18921 (2011).
- [15] J. Z. Wu, Z. H. Ji, Y. C. Zhang, L. R. Wang, Y. T. Zhao, J. Ma, L. T. Xiao, and S. T. Jia, *Opt. Lett.* **36**, 2038 (2011).
- [16] F. P. D. Santos, F. Perales, J. Leonard, A. Sinatra, J. M. Wang, F. S. Pavone, E. Rasel, C. S. Unnikrishnan, and M. Leduc, *Eur. Phys. J. D* **14**, 15 (2001).
- [17] Y. Chen, W. Lin, H. Hsue, L. Hsu, and I. A. Yu, *Chin. J. Phys.* **38**, 920 (2005).
- [18] M. Marinescu and A. Dalgarno, *Z. Phys. D: At., Mol. Clusters* **36**, 239 (1996).
- [19] R. F. Gutterres, M. Argollo de Menezes, C. E. Fellows, and O. Dulieu, *Chem. Phys. Lett.* **300**, 131 (1999).
- [20] M. Marinescu and A. Dalgarno, *Phys. Rev. A* **52**, 311 (1995).
- [21] L. Young, W. T. Hill. III, S. J. Sibener, S. D. Price, C. E. Tanner, C. E. Wieman, and S. R. Leone, *Phys. Rev. A* **50**, 2174 (1994).
- [22] A. Dervianko, J. F. Babb, and A. Dalgarno, *Phys. Rev. A* **63**, 052704 (2001).
- [23] A. Derevianko and S. G. Porsev, *Phys. Rev. A* **65**, 053403 (2002).
- [24] C. Chin, V. Vuletic, A. J. Kerman, S. Chu, E. Tiesinga, P. J. Leo, and C. J. Williams, *Phys. Rev. A* **70**, 032701 (2004) .
- [25] N. Vanhaecke, C. Lisdat, B. T'Jampens, D. Comparat, A. Crubellier, and P. Pillet, *Eur. Phys. J. D* **28**, 351 (2004).